Journal of Medicinal Chemistry

Drug Annotation

pubs.acs.org/jmc

Discovery of a Cyclic Boronic Acid β-Lactamase Inhibitor (RPX7009) with Utility vs Class A Serine Carbapenemases

Scott J. Hecker,*[,†] K. Raja Reddy,[†] Maxim Totrov,[‡] Gavin C. Hirst,[†] Olga Lomovskaya,[†] David C. Griffith,[†] Paula King,[†] Ruslan Tsivkovski,[†] Dongxu Sun,[†] Mojgan Sabet,[†] Ziad Tarazi,[†] Matthew C. Clifton,[§] Kateri Atkins,[§] Amy Raymond,[§] Kristy T. Potts,[§] Jan Abendroth,[§] Serge H. Boyer,[†] Jeffrey S. Loutit,[†] Elizabeth E. Morgan,[†] Stephanie Durso,[†] and Michael N. Dudley[†]

[†]Rempex Pharmaceuticals, Inc., A Subsidiary of The Medicines Company, 3033 Science Park Rd., Suite 200, San Diego, California 92121, United States

[‡]Molsoft L.L.C., 11199 Sorrento Valley Road, San Diego, California 92121, United States

[§]Beryllium, 3 Preston Court, Bedford, Massachusetts 01730, United States

ABSTRACT: The increasing dissemination of carbapenemases in Gram-negative bacteria has threatened the clinical usefulness of the β-lactam class of antimicrobials. A program was initiated to discover a new series of serine β-lactamase inhibitors containing a boronic acid pharmacophore, with the goal of finding a potent inhibitor of serine carbapenemase enzymes that are currently compromising the utility of the carbapenem class of antibacterials. Potential lead structures were screened in silico by modeling into the active sites of key serine β-lactamases. Promising candidate molecules were synthesized and evaluated in biochemical and whole-cell assays. Inhibitors were identified with potent inhibition of serine carbapenemases, particularly the *Klebsiella pneumoniae* carbapenemase (KPC), with no inhibition of mammalian serine proteases. Studies in vitro and in vivo show that RPX7009 (**9f**) is a broad-spectrum inhibitor, notably restoring the activity of carbapenems against KPC-producing strains. Combined with a carbapenem, **9f** is a promising product for the treatment of multidrug resistant Gram-negative bacteria.

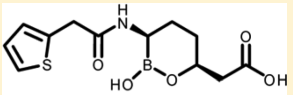

9f

INTRODUCTION

Rapidly rising resistance to multiple antimicrobial agents in Gram-negative bacteria, commonly related to healthcare-associated infections, is an emerging public health concern in U.S. hospitals. While the cephalosporin class of β-lactams was the mainstay of treatment in the 1980s, the dissemination of extended-spectrum β-lactamases (ESBLs) over the past 2 decades has dramatically weakened the utility of this class and brought about a corresponding reliance on the carbapenems.[1] Although carbapenems are widely recognized as a safe and effective class of antimicrobials, carbapenem-resistant Enterobacteriaceae (CRE) due to the *Klebsiella pneumoniae* carbapenemase (KPC) and other β-lactamases now threatens the usefulness of all β-lactam antibiotics.[2] The Centers for Disease Control (CDC) considers CRE to be an urgent antimicrobial resistance threat that now has been detected in nearly every U.S. state, with an alarming increase in incidence over the past 5 years.[3] The failure to develop antimicrobial agents to manage CRE threatens to have a catastrophic impact on the healthcare system.[4]

A proven strategy to overcome resistance to β-lactam antibiotics has been to restore their activity by combining them with an inhibitor of the β-lactamase enzymes responsible for their degradation. Examples of clinically important β-lactamase inhibitors (Figure 1) include clavulanic acid (combined with amoxicillin), sulbactam (with ampicillin), and tazobactam (with piperacillin). The KPC β-lactamase is poorly inhibited by these β-lactamase inhibitors, and thus, they have no usefulness in the treatment of infections due to CRE. More recently, the diazabicyclooctane inhibitors avibactam (NXL-104)[5] and relebactam (MK-7655)[6] have entered clinical development, in combination with ceftazidime and imipenem, respectively. Both compounds display a broad spectrum of β-lactamase inhibition that includes the KPC enzyme.

Boronic acids have long been explored as inhibitors of serine proteases.[7] Mechanistically, the affinity of boronates for serine hydrolases is due to the formation of a covalent adduct between the catalytic serine side chain and the boronate moiety, which effectively mimics the tetrahedral transition state on the acylation or deacylation reaction path. β-Lactamase inhibition by boronic acids such as phenylboronic acid **1** (Figure 2) was first reported from researchers at Oxford University,[8] who noted an earlier observation[9] that borate ions inhibit β-lactamase I. Following publication of the high-resolution X-ray crystal structure of the class A RTEM-1 β-lactamase of *E. coli*,[10] the group of Jones (Toronto) described a rationally designed inhibitor **2** that displayed an inhibition constant of 110 nM.[11,12] Further structure-guided design yielded two highly potent inhibitors **3** and **4** with inhibition constants of 6 and 13 nM, respectively.[13] From the late 1990s to the present, several publications from the laboratory of B. Shoichet detailed structure-based design efforts in this class (e.g., compounds **5** and **6**).[14,15] More recently, published patent applications[16−18] describe analogs (e.g., **7**)

Received: January 22, 2015

DOI: 10.1021/acs.jmedchem.5b00127
J. Med. Chem. XXXX, XXX, XXX−XXX

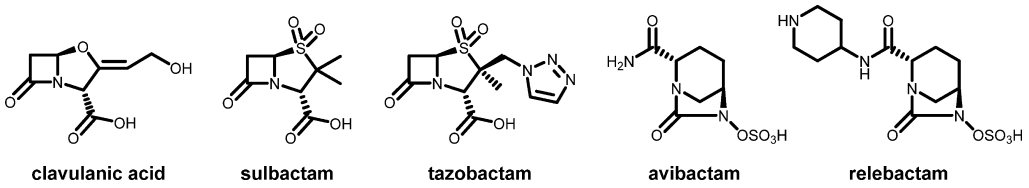

Figure 1. Currently marketed and promising new β-lactamase inhibitors.

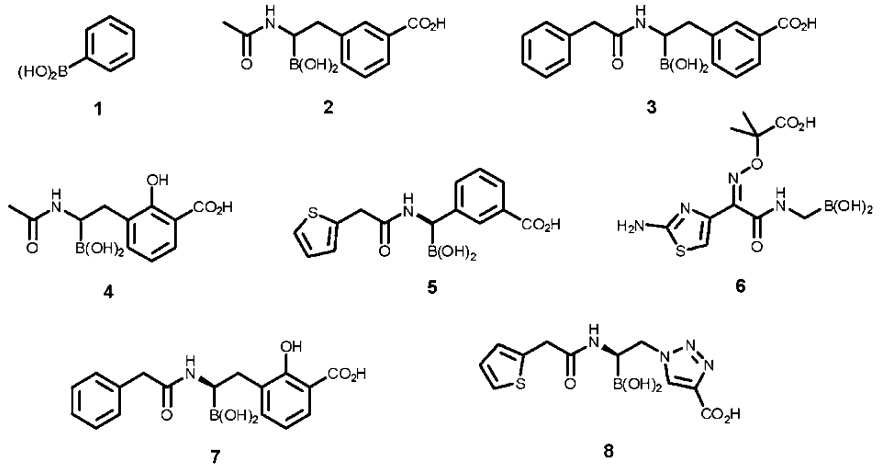

Figure 2. Previously reported boronic acid β-lactamase inhibitors.

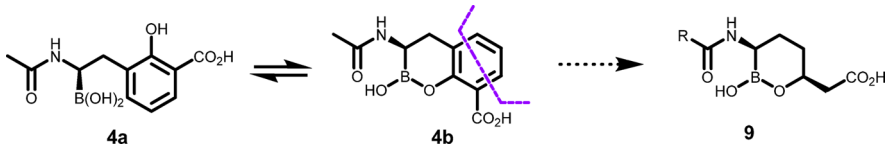

Figure 3. Design of cyclic boronate **9**.

related to earlier compounds **3** and **4**, as well as heterocyclic variants such as **8**[19] (see Figure 2). Notably, despite a high level of interest by multiple investigators, there is not a single report related to determination of efficacy in an animal infection model with any of the compounds of these classes. Believing that boronate-containing β-lactamase inhibitors might find utility in inhibiting the problematic serine carbapenemases of CRE, we set out to identify a potent inhibitor of the KPC enzyme for use in combination with a carbapenem.

DESIGN

Of the various leads explored by others, we were particularly interested in the inhibitors reported by Ness et al.[13] for their high potency in inhibiting some class A β-lactamases. These authors found that installation of a hydroxyl group on the aromatic ring of compound **4a** caused a considerable increase in affinity to the TEM-1 enzyme. They considered the possibility of formation of cyclized variant **4b**; however, they concluded from examination of the X-ray crystal structure of this compound bound to TEM-1 that it existed in the acyclic form (**4a**, Figure 3). We were intrigued by the possibility of using cyclic boronate ester formation to constrain potential lead molecules into the preferred conformation for enzyme complexation. We also anticipated that cyclic boronates may have better selectivity toward β-lactamases versus other serine hydrolases that have linear substrates. The latter enzymes are likely to have more sterically restricted active sites that can accommodate a linear but not a cyclic transition state mimetic inhibitor. Several structures were proposed and were docked in silico with β-lactamase enzymes from classes A, C, and D. Modeling of the precovalent (Michaelis) complex as well as covalent adduct was performed. High affinity of the precovalent complex is expected to facilitate rapid complex formation, while favorable inhibitor/enzyme interactions within the covalent adduct are important to maintain the complex, since the boronate/serine side chain reaction is reversible. On the basis of the docking results, the highest ranking of the proposed inhibitor types was structure **9**, from which the fused benzo ring of **4b** has been excised.

Encouragingly, structure **9** exhibited similar favorable precovalent (free docking) and covalently bound poses in representative class A and C enzyme active sites. Comparison to an available X-ray structure of the Michaelis substrate complex in the active site of AmpC (S64G mutant, Protein Data Bank entry 1KVL)[20] showed that the putative inhibitor could capture key substrate−enzyme interactions (Figure 4). The carboxylate moiety is extensively coordinated within the subpocket that coordinates the carboxylate of the substrate β-lactam. The amide carbonyl forms hydrogen bonds to two hydrogen bond donor groups. The free hydroxyl of the boronic acid moiety enters the oxyanion hole, and the lipophilic portion of the ring engages in hydrophobic interactions with two leucine side chains, again matching the corresponding interactions of the substrate. While no similar experimental structure was available for a class A enzyme/substrate Michaelis complex at the time, our modeling suggested that the inhibitor could also mimic the substrate interactions closely. In contrast to the boron-containing "core,"

DOI: 10.1021/acs.jmedchem.5b00127
J. Med. Chem. XXXX, XXX, XXX−XXX

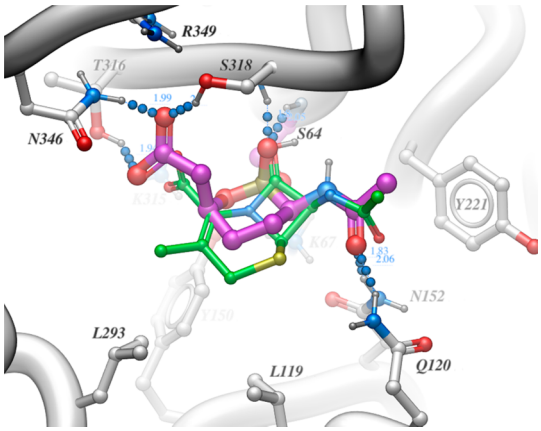

Figure 4. Model of **9** bound at the active site of class C β-lactamase (magenta). X-ray structure of cephalothin (core portion, green) bound to AmpC (enzyme is superimposed) is shown in green. Blue balls represent hydrogen bonds.

the region of the binding site associated with the *N*-acyl substituent was variable across the different serine β-lactamases; it appeared that this region would benefit from a hydrophobic substituent but more specific insights could not be gleaned from the initial model.

SYNTHESIS

The synthesis of cyclic boronates **9a–y** was accomplished in six steps in an overall yield of about 30% (Scheme 1). Enantiopure β-hydroxy ester **10**, prepared by lipase-mediated kinetic resolution of the corresponding racemate,[21] was protected as its silyl ether **11** with TBSCl and imidazole. Regioselective hydroboration with catalysis by $[Ir(COD)Cl]_2$ gave pinacol boronate **12** which was converted to the more stable pinanediol boronate **13**. Stereoselective chloromethylation following Matteson's protocol at −100 °C afforded the (*S*)-chloro homologue **14** as an 85:15 mixture of diastereomers. Stereospecific displacement of the chloro group with hexamethyldisilazide followed by in situ acylation gave acylamidoboronate **15**. Acidic removal of all protecting groups afforded the cyclic boronic ester analogs **9a–r**.

EVALUATION OF ANALOGS

Potentiation of Carbapenems against the KPC-2 Carbapenemase. Initial evaluation of early analogs of **9** quickly established that in addition to submicromolar activity against most serine β-lactamases (vide infra), members of this structure class displayed exceptional activity in inhibition of KPC-type carbapenemase enzymes. It was quickly recognized that inhibition of just this one class of β-lactamase would address a key resistance mechanism that threatens the utility of the carbapenem class. From the outset, we envisioned that our ultimate product would be a combination with either meropenem (because of its excellent safety record and registration status in most of the world) or biapenem (being the least effluxed of the carbapenems in *Pseudomonas aeruginosa* and having the best stability to the metallo β-lactamase NDM-1).

Medicinal chemistry efforts were focused on understanding the structure–activity relationships (SARs) of the *N*-acyl substituent with respect to potentiation of a carbapenem against KPC-producing strains. Results of evaluating the ability of selected inhibitor analogs **9** to potentiate biapenem against a KPC-producing strain of *Klebsiella pneumoniae* (KP1004) are shown in Table 1. Potency is expressed as MPC_1, defined as the minimum concentration of the β-lactamase inhibitor required to reduce the biapenem MIC from 32 μg/mL (no inhibitor) to 1 μg/mL; in addition to KPC-2, KP1004 also produces the β-lactamase enzymes SHV-11 and TEM-1. The simple *N*-acetyl analog **9a** afforded potent activity, with 0.3 μg/mL being sufficient to reduce the biapenem MIC from 32 to 1 μg/mL. In most cases, further substitution had only a modest impact on potency. Whereas phenylacetyl analog **9c** was only 2-fold improved relative to **9a** (MPC_1 = 0.15 μg/mL), the 2-thienyl acetyl analog **9f** (reminiscent of the marketed cephalosporins cephalothin and cefoxitin) was 16-fold more potent than **9a** (MPC_1 = 0.02 μg/mL). Replacement of the thiophene of **9f** by other heterocycles such as aminothiazole (**9g**) or pyridyl (**9i–k**) resulted in lesser activity, although potency was restored by incorporation of an amino group in aminopyridyl analog **9l**

Scheme 1. Synthesis of Cyclic Boronate Analogs 9a–r

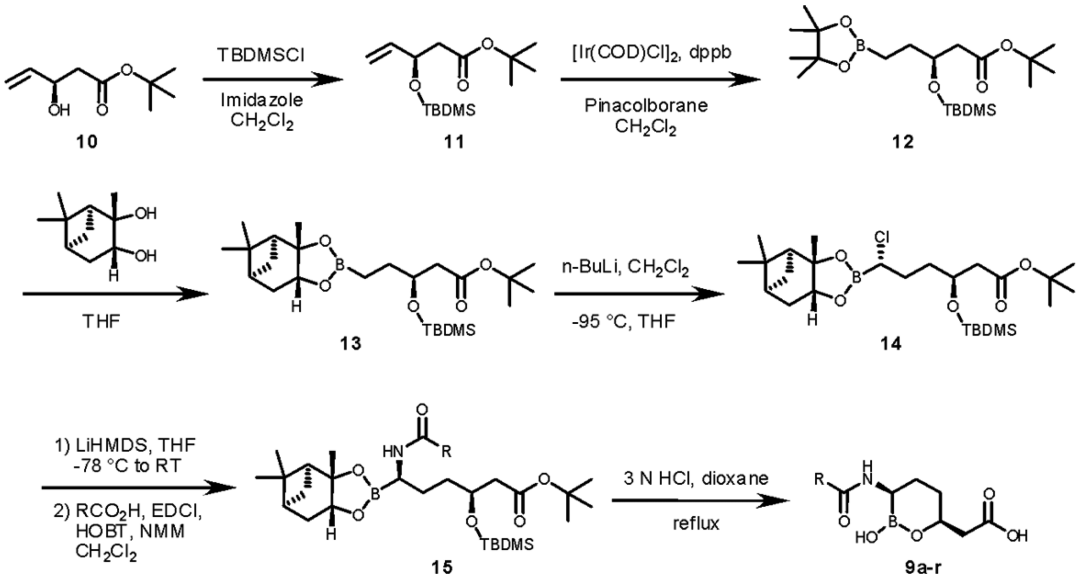

DOI: 10.1021/acs.jmedchem.5b00127
J. Med. Chem. XXXX, XXX, XXX–XXX

Table 1. Potentiation of Biapenem by Members of Inhibitor Analog Series 9

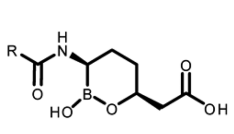

9

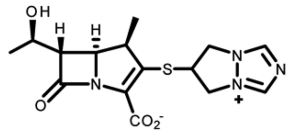

biapenem

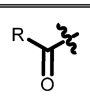		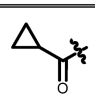	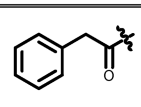	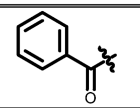	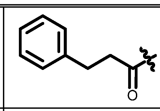	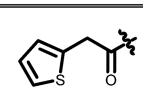
Cmpd #	**9a**	**9b**	**9c**	**9d**	**9e**	**9f**
MPC_1 (μg/mL)	0.30	0.15	0.15	0.30	0.30	0.02
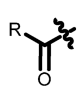	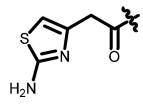	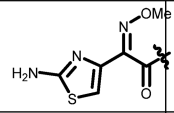	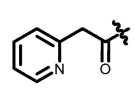	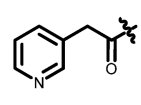	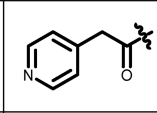	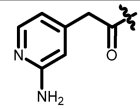
Cmpd #	**9g**	**9h**	**9i**	**9j**	**9k**	**9l**
MPC_1 (μg/mL)	0.61	1.25	0.15	0.15	0.15	0.04
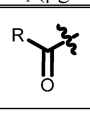	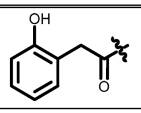	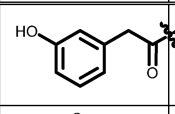	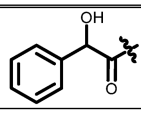	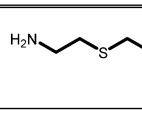	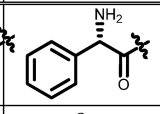	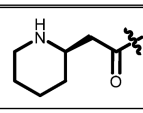
Cmpd #	**9m**	**9n**	**9o**	**9p**	**9q**	**9r**
MPC_1 (μg/mL)	0.16	1.25	0.61	0.30	0.30	0.15

(MPC_1 = 0.04 μg/mL). Various hydroxyl substitutions (**9m**–**o**) and basic groups (**9p**–**r**) were tolerated but offered no advantage. None of these compounds displayed any antibacterial activity when tested in the absence of a β-lactam. At the conclusion of this SAR study, compound **9f** (RPX7009)[22] was selected for further evaluation as a potential development candidate because of its high potency as well as precedent for the thienylacetyl side chain in the marketed cephalosporins cephalothin and cefoxitin.

FURTHER EVALUATION OF COMPOUND 9f IN VITRO

Inhibition of Nitrocefin Degradation. The spectrum of β-lactamase inhibition of **9f** was initially evaluated by measuring inhibition of nitrocefin degradation by purified β-lactamase enzymes.[23] This compound features a broad spectrum of inhibition of β-lactamases, with particularly potent activity against KPC, CTX-M, SHV, and CMY enzymes (Table 2). Notably, **9f** is considerably more potent than the β-lactamase inhibitors clavulanic acid and tazobactam against the class A carbapenemase KPC-2 as well as the class C enzymes P99 and CMY-2.

Whole-Cell Activity in Combination with Cefepime. The spectrum of β-lactamase inhibition was evaluated in whole cells in combination with cefepime (Table 3).[24] Restoration of cefepime activity against various clinical strains expressing serine enzymes from classes A, C, and D is observed. In general, we observed a reasonably good correlation between the biochemical enzyme inhibition results and cellular activity. For example, **9f** has the lowest potency against the TEM-10 enzyme; likewise, the lowest extent of potentiation is observed against strains expressing TEM β-lactamases. Still, in addition to intrinsic potency, other factors most certainly affect the observed extent of potentiation, including rate of uptake and active efflux of the inhibitor as well as the enzyme expression level.

Table 2. Inhibition of Nitrocefin Degradation (K_i, μM) by Compound 9f

enzyme	class	9f	clavulanic acid	tazobactam
KPC-2	A	0.069	41.2	1.6
CTX-M-15	A	0.044	0.027	0.001
SHV-12	A	0.029	≤0.039	0.0004
TEM-10	A	0.110	0.020	0.005
P99	C	0.053	1106	1.10
CMY-2	C	0.099	845	0.71

Whole-Cell Activity in Combination with Carbapenems. The potent inhibition of KPC enzymes by our series of β-lactamase inhibitors along with the intrinsic stability of carbapenems to ESBLs and ampC invited combination of our inhibitors with these antimicrobials. Table 4 illustrates the ability of compound **9f** to potentiate various carbapenem antibiotics against clinical isolates of *Enterobacteriaceae* expressing class A carbapenemases, including strains producing other class A β-lactamases associated with resistance to cephalosporins. It should be noted that these carbapenems are stable to the β-lactamases represented in the strains in Table 3 and thus are highly active on their own against these strains. However, when KPC is present, carbapenem MICs are also affected by mutations in the genes coding for major porins such as Omp35 and OmpK36, and the highest MICs are associated with strains that have double porin mutations (for example, strains KP1084 and KP1087). Even in these strains, compound **9f** is effective in reducing the MICs to susceptible levels.

Selectivity of Protease Inhibition. One concern for inhibitors that interact covalently with β-lactamases was that they might prove to be inhibitors of mammalian serine proteases. Therefore, **9f** was evaluated against a panel of common mammalian serine proteases. As shown in Table 5, IC_{50} values for 11 different mammalian serine proteases were all ≥1000 μM.

DOI: 10.1021/acs.jmedchem.5b00127
J. Med. Chem. XXXX, XXX, XXX−XXX

Table 3. MICs to Cefepime Alone or in Combination with 9f

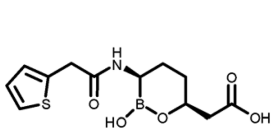

9f (RPX7009)

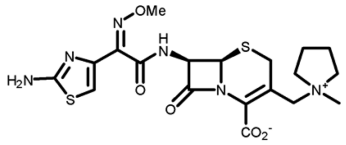

cefepime

organism	strain	enzyme	cefepime MIC (μg/mL)	cefepime MIC with 4 μg/mL **9f** (μg/mL)
Escherichia coli	EC1008	CTX-M-3	>64	4
Klebsiella pneumoniae	KP1005	CTX-M-14	64	4
Klebsiella pneumoniae	KP1009	CTX-M-15	>64	2
Klebsiella pneumoniae	KP1011	SHV-5	64	0.25
Klebsiella pneumoniae	KP1010	SHV-12	2	0.25
Escherichia coli	EC1009	TEM-10	8	4
Escherichia coli	EC1011	TEM-26	8	2
Enterobacter cloacae	ECL1003	TEM, SHV	32	8
Enterobacter cloacae	ECL1002	Hyper AmpC expression	16	0.5
Enterobacter cloacae	ECL1061	Hyper AmpC expression, KPC-3	>64	2
Enterobacter cloacae	EC1010	CMY-6	>64	4
Klebsiella oxytoca	KX1001	OXA-2	4	0.5
Enterobacter aerogenes	EA1028	OXA-30	>64	0.5

Table 4. MIC values (in μg/mL) of Carbapenems in the Presence of Compound 9f (at 4 μg/mL) against Clinical Strains Producing Serine Carbapenemases

			biapenem		meropenem		ertapenem		imipenem	
organism	strain	enzyme	alone	with **9f**	alone	with **9f**	alone	with **9f**	alone	with **9f**
Escherichia coli	EC1007	KPC-3	8	≤0.06	4	≤0.06	8	≤0.06	8	0.13
Enterobacter cloacae	ECL1058	KPC-3, SHV-11, TEM-1	8	≤0.06	8	≤0.06	32	0.25	8	0.25
Klebsiella oxytoca	KX1019	KPC-2, OXA-2	8	0.25	4	≤0.06	16	0.25	4	0.13
Klebsiella oxytoca	KX1017	KPC-2, OXA-2, SHV-30	4	≤0.06	4	≤0.06	16	0.25	8	0.13
Klebsiella pneumoniae	KP1004	KPC-2, TEM-1, SHV-11	8	≤0.06	8	≤0.06	32	≤0.06	8	≤0.06
Klebsiella pneumoniae	KP1008	KPC-2	8	≤0.06	4	≤0.06	8	≤0.06	4	≤0.06
Klebsiella pneumoniae	KP1082	KPC-2, SHV-1	4	≤0.06	4	≤0.06	4	≤0.06	4	0.13
Klebsiella pneumoniae	KP1087	KPC-2, CTX-M-15, SHV-11, TEM-1	16	0.25	64	1	>64	2	16	0.25
Klebsiella pneumoniae	KP1083	KPC-3, SHV-1, TEM-1	16	≤0.06	16	≤0.06	32	≤0.06	16	0.13
Klebsiella pneumoniae	KP1084	KPC-3, SHV-11, TEM-1	64	0.25	>64	0.5	>64	4	64	0.25
Klebsiella pneumoniae	KP1088	KPC-3, SHV-11, TEM-1	32	≤0.06	8	≤0.06	16	≤0.06	32	≤0.06

Table 5. IC_{50} Values (in μM) for Inhibition of Mammalian Serine Proteases by 9f

enzyme	IC_{50} (μM)
trypsin	>1000
chymotrypsin	>1000
plasmin	>1000
thrombin	>1000
elastase	>1000
urokinase	>1000
tissue plasminogen activator (TPA)	>1000
chymase	>1000
Ddipeptidyl peptidase 7 (DPP7)	>1000
neutrophil elastase	>1000
cathepsin A	1000

CRYSTALLOGRAPHY

To fully understand the mechanism of action and gain insights that might influence the design of new inhibitors, we sought to determine the structures of representative members of class A (CTX-M-15) and class C (AmpC) bound to **9f**. The structures of CTX-M-15 and AmpC were solved to 1.5 and 1.7 Å, respectively, in the presence of **9f**. Crystallization conditions are described in the Experimental Section.[25]

Consistent with the design of **9f**, the structures of CTX-M-15 (Figure 5) and AmpC (Figure 6) complexes clearly show that the catalytic serine residue of each enzyme is covalently bound to the boron atom of the inhibitor. The two complexes share several additional common features. In each, the amide moiety of the inhibitor is extensively coordinated, donating a hydrogen bond to the S237/S318 backbone carbonyl and accepting hydrogen bonds from the side chains of N132/N152 and N104/Q120 (CTX-M-15/AmpC residue numbers, respectively). The carboxylate of the ligand is also well-coordinated, by T235/T316, S237/S318, and S130 (CTX-M-15 only) side chain hydroxyls. In the structure of CTX-M-15, the thiophene moiety of **9f** is bound in a single fixed position, whereas in AmpC it has an increased range of motion allowing two unique orientations to be observed. A remarkable difference between the two complexes is the inversion of the six-membered cyclic boronic acid ester ring: both conformations are "chair"; however in the CTX-M-15 complex the amide substituent is in the axial orientation and carboxymethyl is equatorial, while in the AmpC complex the amide is equatorial and carboxymethyl is axial. The conformation of the inhibitor in the AmpC complex allows for a more

DOI: 10.1021/acs.jmedchem.5b00127
J. Med. Chem. XXXX, XXX, XXX−XXX

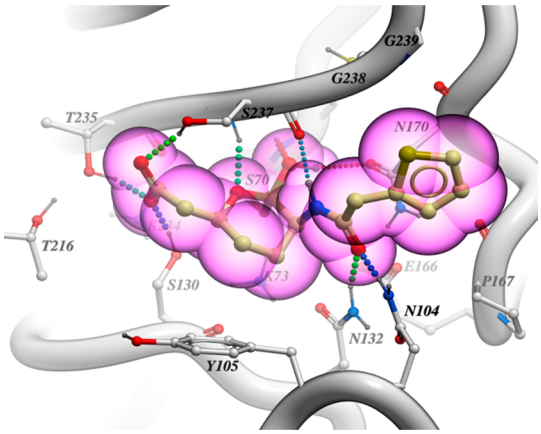

Figure 5. Compound **9f** bound to CTX-M-15.

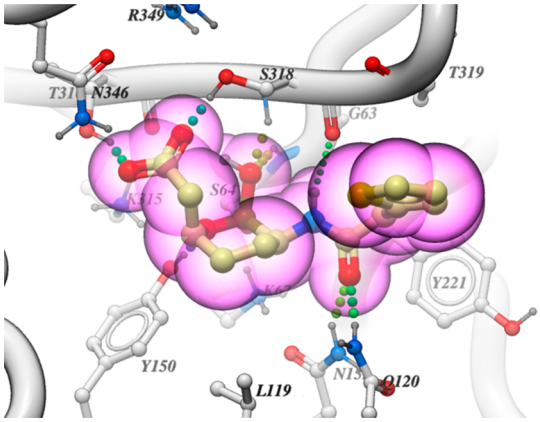

Figure 6. Compound **9f** bound to AmpC.

substrate-like interaction with the enzyme, with the hydroxyl oxygen of the boronate interacting in the oxyanion hole formed by the backbone NH groups of S64 and S318, while the ring oxygen forms a hydrogen bond to the hydroxyl of Y150. These two oxygen atoms likely correspond to the carbonyl oxygen and the nitrogen of the β-lactam substrate, respectively. On the other hand, in the CTX-M-15 complex both oxygen atoms are interacting with the oxyanion hole, which is significantly expanded. The conformation of the ring is likely dependent on the amount and configuration of space available for the two substituents; in CTX-M-15 the amide subpocket is significantly shallower, making axial configuration of the amide sterically preferable, while in AmpC the carboxylate subpocket is oriented more "upwards" from the ring, resulting in axial positioning of the carboxymethyl group. Notably, the ability of the inhibitor to switch between two conformations allows it to retain activity against two different enzyme classes.

We compared the X-ray structures to our earlier models that informed the design. The model of the covalent class C enzyme/**9f** complex was remarkably accurate (rmsd for all heavy atoms, 0.8 Å), with all interactions essentially identical between the X-ray and the model. Interactions in class A enzyme complex were also largely correctly reproduced, although our covalent complex model differed from the X-ray in that the 6-ring was predicted to assume "boat" conformation upon covalent binding, resulting in somewhat higher rmsd of 1.2 Å. In this case our precovalent state model was closer to the experimental (covalent) complex, with rmsd of 1.0 Å. A delicate balance between the lower internal strain of the "chair" conformer and the strength of receptor–ligand interactions likely defines the observed conformation.

EVALUATION OF COMPOUND 9f IN VIVO

Pharmacokinetics. The pharmacokinetics of **9f** were studied in the rat at multiple doses (Table 6).[26] The systemic

Table 6. Mean Pharmacokinetic Parameters of Compound 9f in Rats

parameter	100 mg/kg	300 mg/kg	1000 mg/kg
C_{max} (mg/L)	231	735	2595
$AUC_{(0-\infty)}$ (h·mg/L)	64	239	1037
$t_{1/2}$ (h)	0.42	0.26	0.40
V_d (L/kg)	0.97	0.48	0.55
Cl (L h^{-1} kg^{-1})	1.60	1.26	0.97

exposure, as shown by the C_{max} and AUC values, generally increased in a dose proportional manner. Overall the parameters were similar to those of most β-lactam antibiotics, evidencing high C_{max} and AUC, short half-life, and low volume of distribution.

Efficacy. The enhancement of biapenem and meropenem activity by compound **9f** against a KPC-producing strain of *Klebsiella pneumoniae* was studied in a neutropenic mouse lung infection model (Figure 7).[27] In this model, biapenem at a dose

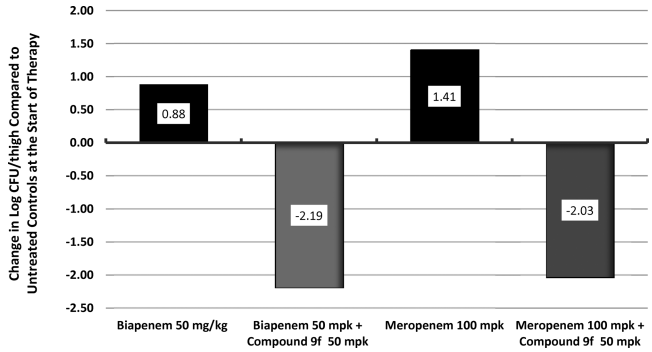

Figure 7. Potentiation of biapenem and meropenem activity by compound **9f** against a carbapenem-resistant strain of *K. pneumoniae* in the neutropenic mouse lung infection model.

of 50 mg/kg and meropenem at a dose of 100 mg/kg are ineffective at reducing viable counts in lung tissue. In combination with biapenem and meropenem, compound **9f** achieved a substantial reduction in viable counts at a dose of 50 mg/kg, attaining over a 2 log colony forming unit (CFU) reduction.

Safety. At doses up to 1000 mg kg^{-1} day^{-1}, compound **9f** exhibited no discernible toxicity in the standard battery of safety pharmacology, repeat-dose toxicology, genotoxicity, and reproductive and developmental toxicity studies.[28]

Phase 1 Pharmacokinetics. The pharmacokinetics of compound **9f** administered as 3 h infusions at doses of 250, 500, 750, 1000, 1250, and 1500 mg were evaluated in a total of 36 normal volunteers.[29] The compound was well-tolerated with no drug-related adverse events. Plasma concentrations were fit to a noncompartmental model; exposures increased proportionally with dose (Figure 8). At the 1 g dose, **9f** displayed a C_{max} of 22.0 μg/mL and a half-life of 1.23 h, the area under the curve (AUC) was 100 μg·h/mL, clearance (Cl) was 12.8 L/h, and the steady-state volume of distribution (V_{ss}) was 21.0 L. These parameters

DOI: 10.1021/acs.jmedchem.5b00127
J. Med. Chem. XXXX, XXX, XXX−XXX

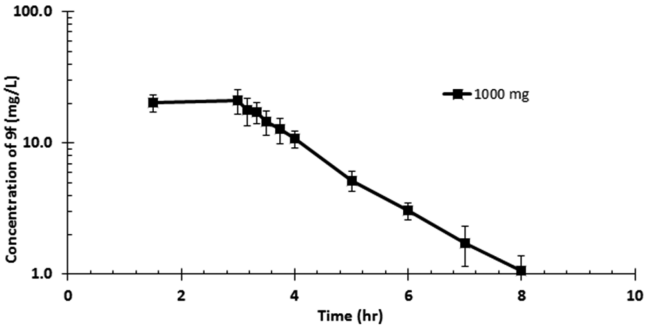

Figure 8. Pharmacokinetic profile of **9f** in normal volunteers following a single 3 h intravenous infusion of 1000 mg.

are similar to those of most β-lactam antibiotics, which are typified by short half-lives and low volumes of distribution.

SUMMARY AND CONCLUSIONS

A program was initiated to discover a potent new inhibitor of β-lactamases for use in treatment of serious Gram-negative infections. In view of the poor activity of currently marketed β-lactamase inhibitors against serine carbapenemases, the program focused on discovery of an inhibitor of these enzymes for combination with a carbapenem antibiotic. On the basis of the boronic acid pharmacophore, a new structure was proposed containing a cyclic α-acylaminoboronic acid. We hypothesized that intramolecular formation of a boronic ester ring would constrain the inhibitor into the preferred conformation for binding, resulting in enhanced potency. Methods for synthesis were developed, relying on the Matteson protocol for access to the key α-chloroboronate species with control of stereochemistry.

Evaluation of initial structures showed achievement of broad-spectrum activity, notably with high potency against the KPC carbapenemase. Variation of the acyl side chain ensued, with a focus on optimizing potency against this key enzyme. Compound **9f** emerged as the most potent analog of this series.

Profiling of **9f** in combination with currently marketed carbapenems showed consistent potentiation against strains with high MICs to the carbapenems alone. In vivo, compound **9f** displays pharmacokinetics in the rat remarkably similar to β-lactam antibiotics including carbapenems. Efficacy against a KPC-producing strain in a neutropenic mouse lung infection model was clearly established. Selectivity for the β-lactamase target was established by screening against a panel of mammalian proteases; IC_{50} values of $\geq$1000 μM were observed. Furthermore, in IND-enabling toxicology studies of **9f** at doses up to 1000 mg kg^{-1} day^{-1}, no adverse effects were observed. In phase 1 studies in healthy volunteers, compound **9f** was well-tolerated, and human pharmacokinetic parameters were as expected based on preclinical species. Patient trials in combination with meropenem are now under way.

EXPERIMENTAL SECTION

General Methods. Unless otherwise noted, solvents and reagents were obtained from commercial suppliers and were used without further purification. All reactions involving air- or moisture-sensitive reagents were performed under an argon atmosphere. Thin-layer chromatography was performed on Merck silica gel 60 plates coated with 0.25 mm layer with fluorescent indicator. Components were visualized by UV light (λ = 254 and 366 nm) and iodine vapors. Column chromatography was conducted either under medium pressure on silica gel (Merck silica gel 40−63 μm) or on prepacked silica gel cartridges (Isco) on an Isco system. The data reported in Table 1 are on 85:15 mixtures of diastereomers; all subsequent data on compound **9f** were obtained on diastereomerically pure material. Other than the presence of the minor diastereomer, the purity of all tested compounds was ≥95%, as determined by HPLC with UV detection at 220 nm. Purity and low-resolution mass spectrometry (MS) data were determined on a ThermoFinnigan Surveyor HPLC and ThermoFinnigan LCQ Advantage instruments equipped with ESI, using an Agilent Eclipse Plus C18 (4.6 mm × 150 mm, 5 μm) column. Mobile phase A was 0.1% trifluoroacetic acid in water, and mobile phase B was 0.1% trifluoroacetic acid in acetonitrile. The following conditions were used: a gradient from 10% to 90% B in 6 min and held at 90% B for 1.5 min; UV detection at 220 and 254 nm; a flow rate of 2 mL/min; an injection volume of 10 μL; full scan, mass range from 100 to 1000 amu. Masses are given as an m/z ratio. ^{1}H NMR spectra were acquired in the indicated solvents on a Bruker NMR spectrometer (Avance TM DRX500, 500 MHz for ^{1}H). Data are reported as the following: chemical shift, multiplicity (s = singlet, d = doublet, t = triplet, q = quartet, bs = broad singlet, dd = doublet of doublet, td = triplet of doublet, m = multiplet), coupling constants, and number of protons.

All experiments utilizing animals were conducted under protocols approved by the Rempex Institutional Animal Care and Use Committee (IACUC). The phase I clinical study was conducted according to Good Clinical Practices (GCP) and met the regulations of the Declaration of Helsinki, the International Conference on Harmonization Good Clinical Practice (E6) guidelines, the United States Food and Drug Administration, and other local regulations and legal requirements. An independent review board and ethics committee approved the study.

(*R*)-*tert*-Butyl 3-(*tert*-Butyldimethylsilyloxy)-pent-4-enoate (11). A 500 mL round-bottom flask equipped with a condenser under argon was charged with (*R*)-*tert*-butyl 3-hydroxy-pent-4-enoate (38.33 g, 0.22 mol) and CH_2Cl_2 (220 mL). Imidazole (22.73 g, 0.33 mol) was added to the solution of alcohol at room temperature. Upon complete dissolution, TBDMSCl (40.25 g, 0.27 mol) was added at once. A white precipitate formed and after a few minutes resulted in a thick slurry. After stirring at room temperature for 1 h, the white slurry was poured into a flask containing a saturated $NaHCO_3$ solution (250 mL) and hexanes (250 mL). After stirring at room temperature for 5 min, the biphasic mixture was poured into a separatory funnel and the layers were separated. The organic layer was washed with a saturated $NaHCO_3$ solution (250 mL), dried (Na_2SO_4), filtered, and concentrated to dryness. The residual tan oil was distilled under reduced pressure (bp 62−54 °C at 0.5 Torr) to give **11** as a colorless oil (59.82 g, 94%); ^{1}H NMR (DMSO-d_6) δ ppm 5.84 (ddd, 1H, J = 17.2, 10.4, 6.0 Hz), 5.21 (dt, 1H, J = 17.2, 1.5 Hz), 5.06 (dt, 1H, J = 10.4, 1.4 Hz), 4.52−4.48 (m, 1H), 2.37 (dd, 1H, J = 14.8, 4.9 Hz), 2.30 (dd, 1H, J = 14.8, 8.0 Hz), 1.39 (s, 9H), 0.84 (s, 9H), 0.04 (s, 3H), 0.02 (s, 3H).

(*S*)-*tert*-Butyl 3-(*tert*-Butyldimethylsilyloxy)-5-(4,4,5,5-tetramethyl[1,3,2]dioxaborolan-2-yl)pentanoate (12). In a round-bottom flask containing a solution of olefin **11** (48 g, 0.17 mol) in CH_2Cl_2 (560 mL) at room temperature were added bis-diphenylphosphinobutane (4.29 g, 10 mmol) and $[Ir(COD)Cl]_2$ (3.38 g, 5 mmol). Upon complete dissolution of the catalyst, pinacolborane (28.8 mL, 0.20 mol) was added to the orange solution. After stirring at room temperature for 4 h, the yellow solution was carefully quenched with MeOH (15 mL). The quenched solution was poured into a separatory funnel and washed with water (250 mL), dried (Na_2SO_4), filtered, and concentrated to dryness. The residual orange oil was purified by column chromatography, eluting with CH_2Cl_2 then hexanes/ethyl acetate 7/3 to give **12** as a colorless oil (66.65 g, 96%); ^{1}H NMR (DMSO-d_6) δ ppm 4.00−3.94−4.48 (m, 1H), 2.31 (dd, 1H, J = 14.8, 4.8 Hz), 2.21 (dd, 1H, J = 14.8, 7.1 Hz), 1.39 (s, 9H), 1.17 (s, 12H), 0.84 (s, 9H), 0.05 (s, 3H), 0.02 (s, 3H).

(3*S*)-*tert*-Butyl 3-(*tert*-Butyldimethylsilyloxy)-5-[(2*S*,6*R*)-2,9,9-trimethyl-3,5-dioxa-4-boratricyclo[6.1.1.0^{2,6}]decan-4-yl)-pentanoate (13). In a round-bottom flask containing a solution of pinacol boronate **12** (22.13 g, 53.4 mmol) in THF (50 mL) was added (+)-pinanediol (10.0 g, 58,7 mmol) at room temperature. After stirring at room temperature for 24 h, the clear colorless reaction mixture was concentrated to dryness and the residual oil was purified by column

DOI: 10.1021/acs.jmedchem.5b00127
J. Med. Chem. XXXX, XXX, XXX−XXX

Table 7. Enzyme Substrates and Buffers Used in the Study

enzyme	buffer	substrate	substrate concn (μM)
trypsin	50 mM Tris-HCl, pH 8.0, 10 mM $CaCl_2$, 100 mM NaCl	N-Bz-R-AMC	200
chymotrypsin	20 mM Tris-HCl, pH 8, 150 mM NaCl, 2.5 mM $CaCl_2$	Suc-AAPF-AMC	10
plasmin	100 mM Tris-HCl, pH 7.5, 100 mM NaCl	H-D-VLK-pNA	200
thrombin	20 mM Tris-HCl, pH 8, 150 mM NaCl, 2.5 mM $CaCl_2$	Benz-FVR-AMC	10
elastase	25 mM Tris-HCl, pH 8.0	Suc-AAPA-pNA	50
urokinase	50 mM Tris HCl, pH 8.5, 38 mM NaCl	NGK-pNA	100
tissue plasminogen activator (TPA)	30 mM Tris-HCl, pH 8.5, 30 mM imidazole, 130 mM NaCl	GK-pNA	100
chymase	100 mM Tris, pH 8.0, 2 M NaCl, 0.01% Triton X-100	Suc-AAPF-AMC	40
dipeptidyl peptidase 7 (DPP7)	50 mM Na-Ac, pH 5.8	H-Lys-Pro-AMC	100
neutrophil elastase	50 mM Tris-HCl, pH 7.5; 1 M NaCl	MeOSuc-AAVP-AMC	30
cathepsin A	25 mM MES, 5 mM DTT, pH 5.5	MCA-RPPGFSAFK-Dnp	10
cathepsin G	50 mM Na-Ac, pH 5.8, 2 mM EDTA, 1 mM DTT	Suc-AAPF-AMC	100
dipeptidyl peptidase 8 (DPP8)	10 mM Tris, pH 7.4, 10 mM $MgCl_2$, 0.05% Tween-20	Lys-Pro-AMC	100
dipeptidyl peptidase 9 (DPP9)	25 mM Tris, pH 7.5, 0.1% BSA	Lys-Pro-AMC	100

chromatography (0−15% ethyl acetate in hexanes) to give **13** as a colorless oil (22.7 g, 91%); ^{1}H NMR (DMSO-d_6) δ ppm 4.29 (dd, 1H, J = 8.6, 1.8 Hz), 4.01−3.98 (m, 1H), 2.33 (dd, 1H, J = 14.8, 4.7 Hz), 2.30−2.25 (m, 1H), 2.22 (dd, 1H, J = 14.8, 7.3 Hz), 2.19−2.13 (m, 1H), 1.95 (t, 1H, J = 5.5 Hz), 1.87−1.83 (m, 1H), 1.7−1.66 (m, 1H), 1.51 (q, 2H, J = 6.0 Hz), 1.39 (s, 9H), 1.31 (s, 3H), 1.24 (s, 3H), 0.99 (d, 1H, J = 10.7 Hz), 0.83 (s, 9H), 0.81 (s, 3H), 0.78−0.64 (m, 2H), 0.04 (s, 3H), 0.02 (s, 3H).

(3*S*,6*S*)-*tert*-Butyl 3-(*tert*-Butyldimethylsilyloxy)-6-chloro-6-[(2*S*,6*R*)-2,9,9-trimethyl-3,5-dioxa-4-boratricyclo[6.1.1.0^{2,6}]-decan-4-yl)hexanoate (14). In a round-bottom flask containing a solution of CH_2Cl_2 (6.9 mL, 107.4 mmol) in THF (150 mL) at −95 °C was added a solution of *n*-BuLi (23.4 mL, 58.6 mmol) along the sides of the flask and keeping the internal temperature below −90 °C. Upon completion of the addition, the reaction mixture was stirred at −95 °C for 30 min. A solution of pinanediol boronate **13** (22.7 g, 48.8 mmol) in THF (40 mL) was added to the solution of dichloromethyllithium, keeping the temperature below −90 °C. Upon completion of the addition, a solution of $ZnCl_2$ in THF (107 mL, 53.7 mmol) was added at −95 °C. The reaction mixture was then allowed to warm to room temperature. After stirring at room temperature overnight, the reaction mixture was quenched with a saturated solution of NH_4Cl, diluted with ethyl acetate (250 mL), and the layers were separated. The organic layer was washed with a saturated solution of NH_4Cl, dried (Na_2SO_4), filtered, and concentrated to dryness. The residual oil was purified by column chromatography to give **14** as a colorless oil (22 g, 88%); ^{1}H NMR (DMSO-d_6) δ ppm 4.41 (dd, 1H, J = 8.7, 1.6 Hz), 4.05 (br p, 1H, J = 5.9 Hz), 3.56 (dd, 1H, J = 8.1, 5.9 Hz), 2.35−2.25 (m, 3H), 2.21−2.16 (m, 1H), 1.99 (t, 1H, J = 5.5 Hz), 1.95−1.82 (m, 2H), 1.65−1.63 (m, 3H), 1.57−1.49 (m, 1H), 1.39 (s, 9H), 1.34 (s, 3H), 1.25 (s, 3H), 1.07 (d, 1H, J = 10.8 Hz), 0.84 (s, 9H), 0.81 (s, 3H), 0.04 (s, 3H), 0.02 (s, 3H).

(3*S*,6*R*)-*tert*-Butyl 3-(*tert*-Butyldimethylsilyloxy)-6-(2-thiophen-2-yl-acetylamino)-6-[(2*S*,6*R*)-2,9,9-trimethyl-3,5-dioxa-4-boratricyclo[6.1.1.0^{2,6}]decan-4-yl)hexanoate (15f). A solution of chloro intermediate **14** (15 g, 29.12 mmol) in THF (145 mL) was cooled to −78 °C under nitrogen. To this solution was slowly added a 1 M solution of LiHMDS in THF (29.1 mL, 29.1 mmol). Upon completion of the addition, the reaction flask was allowed to warm to room temperature. After stirring at room temperature for 16 h, the reaction mixture was concentrated and hexanes (300 mL) was added. The precipitated lithium salts were filtered off, rinsed with hexanes and the combined filtrates were concentrated to give 18 g of crude displacement product.

To a stirred solution of 2-thiopheneacetic acid (4.96 g, 34.94 mmol) in dichloromethane (900 mL) at 0 °C under nitrogen were added EDCI (8.34 g, 43.68 mmol) and HOBT (4.71 g, 34.94 mmol). After stirring at 0 °C for 30 min, a solution of the hexamethyldisilazane displacement product (29.1 mmol) in dichloromethane (70 mL) was added, followed by *N*-methylmorpholine (6.39 mL, 58.24 mmol). Upon completion of the addition, the reaction flask was allowed to warm to room temperature. After stirring at room temperature overnight, the reaction mixture was washed with water, then brine, dried (Na_2SO_4), filtered, and concentrated under vacuum. The residue was purified by column chromatography (gradient of 100% dichloromethane to 40% EtOAc/dichloromethane) to afford amide **15f** as a white solid (12.5 g, 70% yield from **14**); ^{1}H NMR (DMSO-d_6) δ ppm 9.27 (br s, 1H), 7.40 (dd, 1H, J = 5.1, 1.3 Hz), 6.98−6.93 (m, 2H), 4.05−3.98 (m, 2H), 3.79 (s, 2H), 2.4−2.35 (m. 1H), 2.31 (dd, 1H, J = 15.1, 5.0 Hz), 2.25 (dd, 1H, J = 15.1, 7.1 Hz), 2.22−2.15 (m, 1H), 2.05−1.95 (m. 1H), 1.83−1.78 (m, 2H), 1.77−1.73 (m, 1H), 1.64 (br d, 1H, J = 13.9 Hz), 1.56−1.4 (m, 4H), 1.39 (s, 9H), 1.34 (d, 1H, J = 9.8 Hz), 1.23 (s, 3H), 1.21 (s, 3H), 0.83 (s, 9H), 0.80 (s, 3H), 0.03 (s, 3H), 0.02 (s, 3H).

(3*R*,6*S*)-[2-Hydroxy-3-(2-thiophen-2-ylacetylamino)[1,2]oxaborinan-6-yl]acetic Acid (9f). To a solution of amide **15f** (7.5 g, 12.11 mmol) in 1,4-dioxane (25 mL) was added 25 mL of 3 N HCl. The reaction mixture was heated at reflux for 90 min, after which the cooled reaction mixture was diluted with water (25 mL) and extracted with diethyl ether (2 × 75 mL). The aqueous layer was concentrated to afford a sticky residue which was azeotroped with MeCN (3 × 100 mL), dissolved in 20% dioxane−water, and lyophilized to afford a white powder (3.5 g, 97%). This material consisted of an 85:15 mixture of the desired (3*R*,6*S*)-isomer and the (3*S*,6*S*)-isomer (by HPLC and ^{1}H NMR). This material was suspended in ethyl acetate (60 mL). Water (15 mL) was added, and most of the compound appeared to go into the water layer. After sonicating for 5 min, a white precipitate formed. The solid was collected by filtration, washed with ethyl acetate (2 × 16 mL), and dried to give 2.28 g (64%) of **9f** as a white solid; ^{1}H NMR (CD_3OD) δ ppm 7.35 (dd, 1H, J = 5.3, 1.3 Hz), 7.05 (dd, 1H, J = 3.5, 1.3 Hz), 7.0 (dd, 1H, J = 5.2 3.5 Hz), 4.15−4.05 (m, 1H), 3.98 (s, 2H), 2.61 (br d, 1H, J = 3.5 Hz), 2.37 (dd, 1H, J = 14.9, 7.4 Hz), 2.24 (dd, 1H, J = 14.9, 5.8 Hz), 1.74 (br d, 1H, J = 12.1 Hz), 1.66−1.52 (m, 2H), 1.03 (br q, 1H, J = 13.1 Hz); ESIMS found for $C_{12}H_{16}BNO_5S$ m/z 280 (100%) (M − H_2O)$^+$.

Modeling. Structures of representative enzymes of classes A and C were extracted from Protein Data Bank (class A, β-lactamase TOHO, PDB entry 1IYS;[30] class C, β-lactamase CMY-2, PDB entry 1RGY[31]) and prepared for docking in ICM (Molsoft, San Diego, CA). Docking of candidate compound structures was performed using ICM Docking module.[32] The lowest-scoring bound conformation was used for analysis of putative interactions for each candidate structure.

Susceptibility Testing. Clinical strains of Enterobacteriaceae expressing single or multiple β-lactamases from various classes (corresponding genes confirmed by PCR and sequence analysis) were used to evaluate the antibiotic potentiation activity of **9f**. MICs were determined using Clinical and Laboratory Standards Institute (CLSI) broth microdilution methods as described in CLSI document M07-A9 (2012).[33] Cefepime or carbapenem MICs were determined in combination with **9f** at a fixed concentration of 4 μg/mL.

Determination of K_i Values on Inhibition of β-Lactamases. K_i values of inhibition of β-lactamases purified from overexpressing

DOI: 10.1021/acs.jmedchem.5b00127
J. Med. Chem. XXXX, XXX, XXX−XXX

recombinant *E. coli* strains were determined spectrophotometrically using nitrocefin (NCF) as reporter substrate. Enzymes were mixed with inhibitors at varying concentrations in reaction buffer (50 mM Na phosphate, pH 7.0, 0.1 mg/mL BSA) and incubated for 10 min at room temperature. 50 μM NCF was added, and substrate cleavage profiles were recorded at 490 nm every 10 s for 10 min on SpectraMax plate reader. K_i values were calculated by method of Waley SG.[34]

Effect of 9f on Serine Proteases. All enzymes and substrates were from commercial sources, and testing was performed according to the manufacturer's protocols with some modifications. Briefly, 50 μL of the diluted enzyme was mixed with 50 μL of an inhibitor at various concentrations and 50 μL of a corresponding buffer (Table 7). Reaction mixtures were incubated for 10 min at 37 °C. Subsequently, 50 μL of corresponding substrate (Table 7) was added and absorbance or fluorescence was monitored for 30 min on a SpectraMax M2 plate reader (Molecular Devices). 4-(2-Aminoethyl)benzenesulfonyl fluoride hydrochloride (AEBSF) and leupeptin were used as positive controls. Rates of reaction were calculated and presented relative to "no treatment" control. IC_{50} values were calculated based on inhibitor concentration producing 50% of enzyme inhibition.

Pharmacokinetic Studies in Rats. After acclimation, rats (n = 3/dose level) were administered single intravenous infusions of **9f** at 100, 300, or 1000 mg/kg. Doses were infused over 0.5 h via an indwelling femoral vein cannula. Plasma (~0.3 mL) samples were collected from each rat at designated time points up to 24 h. Blood samples were centrifuged within 5 min of collection at 12 000g for 5 min to obtain plasma. The plasma samples were analyzed using an HPLC−MS method. PK analysis was performed using WinNonlin.

Mouse Efficacy Studies. Swiss Webster mice were rendered neutropenic by the administration of cyclophosphamide and were infected under isoflurane anesthesia by intratracheal administration of strain KP1074 (biapenem MIC = 64 μg/mL; biapenem MIC = 0.25 μg/mL in the presence of 4 μg/mL **9f**; meropenem MIC = 128 μg/mL; meropenem MIC = 1.0 μg/mL in the presence of 4 μg/mL **9f**). Treatments were given every 2 h by the intraperitoneal route, starting 2 h postinfection. Animals were sacrificed 24 h after the start of treatment, and the lungs were removed, homogenized, and plated to determine bacterial counts.

Construct Design and Expression. AmpC from *E. cloacae* (GenBank entry X07274.1, residues 21−381) and CMX-M-15 from *K. pneumoniae* (GenBank entry AAY46940.1, residues 29−291) were each cloned using standard restriction enzyme cloning techniques into a pET28 vector modified with a N-terminal 6× histidine-Smt tag. Ligation products were transformed into Top10 *E. coli* cells and plated on 2YT agar in the presence of 50 μg/mL kanamycin. Single colonies of AmpC and CMX-M-15 were grown overnight under antibiotic selection in 2YT media. Cells were harvested, and the plasmid DNA was isolated using a mini-prep kit. All final constructs were sequence verified. A starter culture containing 50 μg/mL (final concentration) kanamycin (Teknova) was inoculated with a single colony and grown for 16 h at 37 °C. This was then transferred to 8 L of terrific broth (Teknova) containing 50 μg/mL (final concentration) kanamycin and grown to OD_{600} = 0.8. Protein expression was induced by adding 1 mM IPTG (VWR) and grown for 16 h at 37 °C. The cells were harvested by centrifugation (Beckman) at 5000 rpm for 15 min, and the pellets were collected and stored at −80 °C.

Protein Purification. Cells were resuspended 1g/4 mL in 25 mM Tris-HCl, pH 8.0, 200 mM NaCl, 0.5% glycerol, 0.02% CHAPS, 10 mM imidazole, 50 mM L-arginine, 1 mM TCEP, 125 U of benzonase, 100 mg of lysozyme, and one complete EDTA free protease inhibitor tablet (Roche). The cells were lysed via sonication (Misonix) and clarified via centrifugation at 45 000 rpm for 30 min at 4 °C and filtered with a 0.2 μm bottle top filter. The supernatant was applied to two 5 mL Ni^{2+} charged HiTrap chelating HP (GE Healthcare) columns, and the protein eluted with a 500 mM imidazole gradient over 24 column volumes. The fractions of interest were pooled, and the His-Smt tag was removed via cleavage with ubiquitin-like-specific protease 1 (Ulp-1) while dialyzing against 2 L of 25 mM Tris, pH 8.0, 200 mM NaCl, 10 mM imidazole, 1 mM TCEP, 50 mM L-arginine, and 0.25% glycerol overnight at 4 °C utilizing 10 000 MWCO snakeskin dialysis tubing. The affinity tag was removed by applying the digested pool over two 5 mL Ni^{2+} charged HiTrap chelating HP columns. The flow through contained the cleaved protein of interest. The protein was concentrated for crystallography via centrifugal concentration (Amicon Regenerated Cellulose, 10 kDa MWCO, Millipore) to 30 mg/mL for both CTX-M-15 and AmpC.

Table 8. X-ray Data Processing Statistics

protein:	AmpC	CTX-M-15
ligand:	**9f**	**9f**
	Data Collection and Processing	
radiation source	ALS 5.0.3	APS 21ID-G
wavelength (Å)	0.9765	0.9786
space group	$P22_12_1$	$P2_12_12_1$
unit cell	62.6 Å, 69.6 Å, 76.3 Å, 90°, 90°, 90°	44.8 Å, 45.8 Å, 116.9 Å, 90°, 90°, 90°
resolution (Å)	50−1.75 (1.8−1.75)	50−1.5 (1.54−1.5)
I/σ	20.0 (4.48)	27.6 (7.64)
completeness (%)	100 (100)	98.7 (98.2)
R_{merge}	0.10 (0.46)	0.03 (0.13)
unique reflections	34340 (2503)	38972 (2806)
multiplicity	7.9 (7.3)	3.9 (3.0)
	Refinement	
R_{cryst} (%)	15.4	13.2
R_{free} (%)	18.6	14.7
rmsd bonds (Å)	0.01	0.01
rmsd angles (deg)	1.57	1.34
mean B-factor (Å^2)	9.67	9.42
	Validation	
Ramachandran favored (%)	98.3	98.5
Ramachandran allowed (%)	0.0	0.4
MolProbity score	0.83 (100th)	0.84 (99th)
Clash score	1.08 (99th)	1.21 (100th)

Crystallization and Structure Determination (Table 8). Compound **9f** was dissolved in DMSO as a 10 mM stock solution and stored at −20 °C. To load the protein prior to crystallization, 5 μL of ligand was added to 50 μL of protein and mixed gently. These samples were allowed to incubate at room temperature for approximately 5 min before gently mixing again and setting up the crystallization experiments. The final concentration of ligand was ~0.9 mM. Crystal trays for both AmpC and CTX-M-15 were set with 100 μL wells and crystal drops containing 0.4 μL of protein (premixed with ligand) and 0.4 μL of crystallant. Crystallization trays were stored at 18 °C, and crystals appeared in 3−20 days. AmpC was crystallized at 30 mg/mL in sitting drop vapor diffusion trays containing a solution comprising 30% PEG 3000, 200 mM NaCl, and 100 mM Tris HCl, pH 7.0. CTX-M-15 was crystallized at at 30 mg/mL in sitting drop vapor diffusion trays containing a solution comprising 2.4 M ammonium sulfate and 100 mM bice NaOH, pH 9.0. Crystals for both proteins were cryoprotected using 20% ethylene glycol and flash frozen with liquid nitrogen. Data for AmpC were collected at the Advanced Light Source in Berkely, CA (ALS), and data for CTX-M-15 were collected at the Advanced Photon Source in Argonne, IL (APS). The data were reduced using XDS[35] and prepared using the Collaborative Computational Project Number 4 (CCP4) suite of programs.[36] Phases were determined by molecular replacement[37] using PDB entry 1XX2 as a search model for AmpC and PDB entry 1IYS as a search model for CTX-M-15. The structures were refined using Refmac,[38] and model building was performed with Coot.[39] The structures were validated using MolProbity.[40]

DOI: 10.1021/acs.jmedchem.5b00127
J. Med. Chem. XXXX, XXX, XXX−XXX

■ ASSOCIATED CONTENT

Accession Codes

Protein Data Bank codes are the following: AmpC/**9f**, 4XUX; CTX-M-15/**9f**, 4XUZ.

■ AUTHOR INFORMATION

Corresponding Author

*Phone: 858-875-6678. E-mail: scott.hecker@themedco.com.

Notes

The authors declare no competing financial interest.

■ ACKNOWLEDGMENTS

Chemistry efforts were supported by Acme Bioscience, Palo Alto, CA. The Berkeley Center for Structural Biology is supported in part by the National Institutes of Health, National Institute of General Medical Sciences, and the Howard Hughes Medical Institute. The Advanced Light Source is supported by the Director, Office of Science, Office of Basic Energy Sciences, of the U.S. Department of Energy under Contract DE-AC02-05CH11231. Use of the Advanced Photon Source, an Office of Science User Facility operated for the U.S. Department of Energy (DOE) Office of Science by Argonne National Laboratory, was supported by the U.S. DOE under Contract DE-AC02-06CH11357. Use of the LS-CAT Sector 21 was supported by the Michigan Economic Development Corporation and the Michigan Technology Tri-Corridor (Grant 085P1000817).

■ ABBREVIATIONS USED

KPC, *Klebsiella pneumoniae* carbapenemase; ESBL, extended spectrum β-lactamase; CRE, carbapenem-resistant *Enterobacteriaceae*; CDC, Centers for Disease Control; MIC, minimum inhibitory concentration; MPC, minimum potentiating concentration; SAR, structure−activity relationship; rmsd, root-mean-square deviation; AUC, area under the curve; Cl, clearance; V_d, volume of distribution; V_{ss}, steady-state volume of distribution; CFU, colony-forming unit; IND, investigational new drug application

■ REFERENCES

(1) Lynch, J. P.; Clark, N. M.; Zhanel, G. G. Evolution of antimicrobial resistance among Enterobacteriaceae (focus on extended spectrum β-lactamases and carbapenemases). *Expert Opin. Pharmacother.* **2013**, *14* (2), 199−210.

(2) Nordmann, P.; Dortet, L.; Poirel, L. Carbapenem resistance in Enterobacteriaceae: here is the storm. *Trends Mol. Med.* **2012**, *18* (5), 263−272.

(3) Centers for Disease Control (CDC) Web site, 2014.

(4) Watkins, R. R.; Bonomo, R. A. Increasing prevalence of carbapenem-resistant Enterobacteriaceae and strategies to avert a looming crisis. *Expert Rev. Anti-Infect. Ther.* **2013**, *11* (6), 543−545.

(5) Zhanel, G. G.; Lawson, C. D.; Adam, H.; Schweizer, F.; Zelenitsky, S.; Lagace-Wiens, P. R. S.; Denisuik, A.; Rubinstein, E.; Gin, A. S.; Hoban, D. J.; Lynch, J. P., 3rd; Karlowsky, J. A. Ceftazidime-avibactam: a novel cephalosporin/β-lactamase inhibitor combination. *Drugs* **2013**, *73* (2), 159−177.

(6) Livermore, D. M.; Warner, M.; Mushtaq, S. Activity of MK-7655 combined with imipenem against Enterobacteriaceae and Pseudomonas aeruginosa. *J. Antimicrob. Chemother.* **2013**, *68* (10), 2286−2290.

(7) Smoum, R.; Rubinstein, A.; Dembitsky, V. M.; Srebnik, M. Boron containing compounds as protease inhibitors. *Chem. Rev.* **2012**, *112* (7), 4156−4220.

(8) Kiener, P. A.; Waley, S. G. Reversible inhibitors of penicillinases. *Biochem. J.* **1978**, *169* (1), 197−204.

(9) Dobozy, O.; Mile, I.; Ferencz, I.; Csanyi, V. Effect of electrolytes on the activity and iodine sensitivity of penicillinase from *B. cereus*. *Acta Biochim. Biophys. Acad. Sci. Hung.* **1971**, *6* (2), 97−105.

(10) Strynadka, N. C.; Adachi, H.; Jensen, S. E.; Johns, K.; Sielecki, A.; Betzel, C.; Sutoh, K.; James, M. N. Molecular structure of the acyl-enzyme intermediate in beta-lactam hydrolysis at 1.7 A resolution. *Nature* **1992**, *359* (6397), 700−705.

(11) Martin, R.; Jones, J. B. Rational design and synthesis of a highly effective transition state analog inhibitor of the RTEM-1 β-lactamase. *Tetrahedron Lett.* **1995**, *36* (46), 8399−8402.

(12) Strynadka, N. C.; Martin, R.; Jensen, S. E.; Gold, M.; Jones, J. B. Structure-based design of a potent transition state analogue for TEM-1 beta-lactamase. *Nat. Struct. Biol.* **1996**, *3* (8), 688−695.

(13) Ness, S.; Martin, R.; Kindler, A. M.; Paetzel, M.; Gold, M.; Jensen, S. E.; Jones, J. B.; Strynadka, N. C. Structure-based design guides the improved efficacy of deacylation transition state analogue inhibitors of TEM-1 beta-lactamase. *Biochemistry* **2000**, *39* (18), 5312−5321.

(14) Morandi, F.; Caselli, E.; Morandi, S.; Focia, P. J.; Blazquez, J.; Shoichet, B. K.; Prati, F. Nanomolar inhibitors of AmpC beta-lactamase. *J. Am. Chem. Soc.* **2003**, *125* (3), 685−695.

(15) Wang, X.; Minasov, G.; Blazquez, J.; Caselli, E.; Prati, F.; Shoichet, B. K. Recognition and resistance in TEM beta-lactamase. *Biochemistry* **2003**, *42* (28), 8434−8444.

(16) Burns, C. J.; Jackson, R. W. Beta-lactamase inhibitors. WO2009064413A1, 2009.

(17) Burns, C. J.; Jackson, R. W.; Goswami, R.; Xu, H. Beta-lactamase inhibitors. WO2009064414A1, 2009.

(18) Burns, C. J.; Goswami, R.; Jackson, R. W.; Lessen, T.; Li, W.; Pevear, D.; Tirunahari, P. K.; Xu, H. Beta-lactamase inhibitors. WO2010130708A1, 2010.

(19) Prati, F.; Caselli, E. Boronic acid inhibitors of beta-lactamases as therapeutic agents in treatment of antibiotic-resistant infection diseases. WO2013053372A1, 2013.

(20) Beadle, B. M.; Trehan, I.; Focia, P. J.; Shoichet, B. K. Structural milestones in the reaction pathway of an amide hydrolase: substrate, acyl, and product complexes of cephalothin with AmpC beta-lactamase. *Structure* **2002**, *10* (3), 413−424.

(21) Vrielynck, S.; Vandewalle, M.; Garcia, A. M.; Mascarenas, J. L.; Mourino, A. A chemoenzymic synthesis of A-ring key-intermediates for 1α,25-dihydroxyvitamin D3 and analogs. *Tetrahedron Lett.* **1995**, *36* (49), 9023−9026.

(22) (a) Hirst, G.; Reddy, R.; Hecker, S.; Totrov, M.; Griffith, D. C.; Rodny, O.; Dudley, M. N.; Boyer, S. Cyclic boronic acid ester derivatives and therapeutic uses thereof. WO2012021455A1, 2012. (b) Hecker, S. J.; Reddy, K. R.; Totrov, M.; Hirst, G. C.; Lomovskaya, O.; Griffith, D. C.; King, P.; Tsivkovski, R.; Sun, D.; Sabet, M.; Tarazi, Z.; Dudley, M. N. Discovery of RPX7009, a broad-spectrum beta-lactamase inhibitor with utility vs. class A serine carbapenemases. Presented at the 52nd International Conference on Antimicrobial Agents and Chemotherapy, San Francisco, CA, 2012; No. F-848.

(23) Tsivkovski, R.; Griffith, D. C.; Hecker, S. J.; Dudley, M. N.; Lomovskaya, O. Biochemical characterization of the beta-lactamase inhibitor RPX7009. Presented at the 52nd Interscience Conference on Antimicrobial Agents and Chemotherapy, San Francisco, CA, 2012; No. F-849.

(24) King, P.; Sun, D.; Griffith, D. C.; Hecker, S. J.; Dudley, M. N.; Lomovskaya, O. Microbiological characterization of beta-lactamase inhibitor RPX7009. Presented at the 52nd Interscience Conference on Antimicrobial Agents and Chemotherapy, San Francisco, CA, 2012; No. F-850.

(25) Clifton, M. C.; Raymond, A.; Atkins, K.; Abendroth, J.; Totrov, M.; Tsivkovski, R.; Hecker, S. J.; Lomovskaya, O. The broad-spectrum serine beta-lactamase inhibitor RPX7009 binds covalently to active site serine residues in CTX-M-15 and AmpC. Presented at the 53rd Interscience Conference on Antimicrobial Agents and Chemotherapy, Denver, CO, 2013; No. F-1199.

(26) Griffith, D. C.; Sabet, M.; Tarazi, Z.; Nolan, T.; Lomovskaya, O.; Hecker, S. J.; Dudley, M. N. Pharmacokinetics of the new beta-lactamase inhibitor RPX7009 in preclinical species. Presented at the 52nd

DOI: 10.1021/acs.jmedchem.5b00127
J. Med. Chem. XXXX, XXX, XXX−XXX

Interscience Conference on Antimicrobial Agents and Chemotherapy, San Francisco, CA, 2012; No. F-851.
(27) Sabet, M.; Tarazi, Z.; Lomovskaya, O.; Hecker, S. J.; Dudley, M. N.; Griffith, D. C. In vivo efficacy of the beta-lactamase inhibitor RPX7009 combined with the carbapenem RPX2003 against KPC-producing K. pneumoniae. Presented at the 52nd Interscience Conference on Antimicrobial Agents and Chemotherapy, San Francisco, CA, 2012; No. F-858.
(28) Griffith, D. C.; Sabet, M.; Tarazi, Z.; Tsivkovski, R.; Lomovskaya, O.; Hecker, S. J.; Dudley, M. N. Nonclinical toxicology and safety profile of the beta-lactamase inhibitor RPX7009. Presented at the 52nd Interscience Conference on Antimicrobial Agents and Chemotherapy, San Francisco, CA, 2012; No. F-852.
(29) Griffith, D. C.; Loutit, J. S.; Morgan, E. E.; Durso, S.; Dudley, M. N. A phase 1 study of the safety, tolerability, and pharmacokinetics of the beta-lactamase inhibitor RPX7009 in healthy adult subjects. Presented at the 24th European Congress of Clinical Microbiology and Infectious Diseases, Barcelona, Spain, 2014; No. eP454.
(30) Ibuka, A. S.; Ishii, Y.; Galleni, M.; Ishiguro, M.; Yamaguchi, K.; Frere, J. M.; Matsuzawa, H.; Sakai, H. Crystal structure of extended-spectrum beta-lactamase Toho-1: insights into the molecular mechanism for catalytic reaction and substrate specificity expansion. *Biochemistry* **2003**, *42* (36), 10634−10643.
(31) Nukaga, M.; Kumar, S.; Nukaga, K.; Pratt, R. F.; Knox, J. R. Hydrolysis of third-generation cephalosporins by class C beta-lactamases. Structures of a transition state analog of cefotoxamine in wild-type and extended spectrum enzymes. *J. Biol. Chem.* **2004**, *279* (10), 9344−9352.
(32) Totrov, M.; Abagyan, R. Flexible protein-ligand docking by global energy optimization in internal coordinates. *Proteins* **1997**, *Suppl 1*, 215−220.
(33) *Methods for Dilution Antimicrobial Susceptibility Tests for Bacteria That Grow Aerobically*, 9th ed.; M07-A9, Vol. 32, No. 2; Clinical and Laboratory Standards Institute: Wayne, PA, 2012; pp 1−68.
(34) Waley, S. G. A quick method for the determination of inhibition constants. *Biochem. J.* **1982**, *205* (3), 631−633.
(35) Kabsch, W. XDS. *Acta Crystallogr., Sect. D: Biol. Crystallogr.* **2010**, *66* (Part 2), 125−132.
(36) Collaborative Computational Project Number 4. The CCP4 suite: programs for protein crystallography. *Acta Crystallogr., Sect. D: Biol. Crystallogr.* **1994**, *50* (Part 5), 760−763.
(37) McCoy, A. J. Solving structures of protein complexes by molecular replacement with Phaser. *Acta Crystallogr., Sect. D: Biol. Crystallogr.* **2007**, *63* (Part 1), 32−41.
(38) Murshudov, G. N.; Vagin, A. A.; Dodson, E. J. Refinement of macromolecular structures by the maximum-likelihood method. *Acta Crystallogr., Sect. D: Biol. Crystallogr.* **1997**, *53* (Part 3), 240−255.
(39) Emsley, P.; Lohkamp, B.; Scott, W. G.; Cowtan, K. Features and development of Coot. *Acta Crystallogr., Sect. D: Biol. Crystallogr.* **2010**, *66* (Part 4), 486−501.
(40) Chen, V. B.; Arendall, W. B., 3rd; Headd, J. J.; Keedy, D. A.; Immormino, R. M.; Kapral, G. J.; Murray, L. W.; Richardson, J. S.; Richardson, D. C. MolProbity: all-atom structure validation for macromolecular crystallography. *Acta Crystallogr., Sect. D: Biol. Crystallogr.* **2010**, *66* (Part 1), 12−21.

DOI: 10.1021/acs.jmedchem.5b00127
J. Med. Chem. XXXX, XXX, XXX−XXX